Progress In Electromagnetics Research B, Vol. 48, 23–42, 2013

LOW-GRAZING ANGLE TARGET DETECTION AND SYSTEM CONFIGURATION OF MIMO RADAR

Jincan Ding*, Haowen Chen, Hongqiang Wang, Xiang Li, and Zhaowen Zhuang

Research Institute of Space Electronics Information Technology, Electronics Science and Engineering School, National University of Defense Technology, Changsha 410073, P. R. China

Abstract—In this paper, we focus on target detection and system configuration optimization of Multiple-input Multiple-output (MIMO) radar in low-grazing angle, where the multipath effects are very abundant. The performance of detection can be improved via utilizing the multipath echoes. First, the reflection coefficient, considering the curved earth effect, is derived. Then, the general signal model for MIMO radar is introduced for low-grazing angle. Using the Neyman-Pearson sense, the detector of MIMO radar with multipath is analyzed. We use the deflection coefficient as a criterion of system configuration both for MIMO radar and phased-array radar. The simulation results show that the performance can be enhanced markedly when the multipath effects are considered, and the optimal configuration of phased-array radar is with the same number of transmitters as that of receivers, however, the optimal configuration of MIMO radar depends on the signal-to-noise ratio (SNR).

1. INTRODUCTION

Over the last decade, the multiple-input multiple-output (MIMO) approach for radar processing has drawn a great deal of attention from researchers and has been applied to various radar scenarios and problems. MIMO radar is categorized into two classes: statistical MIMO radar and colocated MIMO radar, depending on their antenna placement [1–6]. The advantages of MIMO radar with collocated antennas have been studied extensively, which include improved detection performance and higher resolution [7], higher sensitivity for

Received 2 December 2012, Accepted 11 January 2013, Scheduled 18 January 2013
* Corresponding author: Jincan Ding (dingjincan@yahoo.cn).

detecting moving targets [8, 9], and increased degrees of freedom for transmission beamforming [10]. MIMO radar with widely separated antennas can capture the spatial diversity of the target's radar cross section (RCS) [11]. This spatial diversity provides the radar systems with the ability to support to high resolution target localization [12], and tracking performance [13].

Much published literature has concerned the issue of MIMO radar detection. Fishler et al. focused on the application of the target spatial diversity to improve detection performance and demonstrated that statistical MIMO radar provided great improvements over other types of array radars [14]. For low-grazing angle detection of MIMO radar, the authors in [15] utilized the time reversal technique in a multipath environment to achieve high target detectability. It was demonstrated that the improved target detectability can be obtained, compared with the commonly used statistical MIMO strategy.

Low-grazing angle targets are difficult to detect, which is one of the great threats propelling radar development. Otherwise, detecting low-altitude targets is of great significance to counter low-altitude air defence penetration. However, up to now, this problem has not been effectively resolved. Multipath effect plays an important role on the low-altitude target detection, by which the target echo signal is seriously polluted, even counteracted [16]. Two aspects can be considered for multipath: suppressing multipath and utilizing it. In a statistical sense, the detection may be enhanced by use the multipath [17]. In [18], the authors investigated the problem of detecting a moving target by exploiting multipath reflections. Other areas of application in which multipath effects are of primary interest are in low-angle tracking [19–21].

The system configuration of MIMO radar is still an open problem, and the good system architecture is the basis of good performance. In [22], the optimal antenna placement is discussed based on Cramer-Rao bound (CRB) for velocity estimation using separated MIMO radar. Assuming all antennas located equidistant from the target, it is shown that symmetrically placing the transmit and receive antennas is the best choice, and the optimal achievable performance is not affected by the relative position of the transmit and receive antennas under and orthogonal received signal assumption. In [23], the authors presented a new framework of the ambiguity function for a bistatic MIMO radar. In [24], the waveform design methods for the optimization the CRB matrix was discussed, under a total power constraint. In [25], the authors used the relative entropy as the criterion of the configuration optimization both for MIMO radar systems and phased-array radar. Some interesting results are presented. For phased-array radar, when

the total numbers of transmitters and receivers are fixed, we should always make the number of transmitters equal to the number of receivers. For MIMO radar, we should use a small number of transmitters in low signal noise ration (SNR) region, and make the number of transmitters equal to the number of receivers in high SNR region.

In this paper, we consider the low-grazing angle target detection in multipath environment for MIMO radar, and compare the detection performance of the case considering multipath effect with the one without multipath effect. We use the deflection coefficient as the criterion of the configuration design both for MIMO radar systems and phased-array radar, and consider the configuration optimization of the number of the transmitters and receivers for both MIMO radar and phased-array radar.

Notation: We list here some notational convention that will be used throughout this paper. We use boldface lowercase letters for vectors and boldface uppercase letters for matrices. The operation of transposition is denoted by superscript T. The symbol $\odot$ represents the Hadamard product. The symbol $\mathrm{diag}\{\mathbf{a}\}$ denotes a diagonal matrix with its diagonal given by the vector $\mathbf{a}$. We let $\mathbf{I}_N$ denote the identity matrix of size $N \times N$. Finally, the symbols $E\{\cdot\}$ and $\mathrm{var}\{\cdot\}$ denote the expected and variance value of a random quantity, respectively, and $|\cdot|$ denotes the absolute operation.

2. PROBLEM FORMULATION

A point source at a distance of R_d from the receiver is considered. If the source is assumed to be a narrowband signal, it can be represented by

$$x(t) = ae^{j(\omega t+\varphi)} \tag{1}$$

where a is the amplitude, ω the angular frequency, and φ the initial phase. In the presence of multipath, the received signals by each receiver consist of two components, namely, the direct and indirect signal. For a simple multipath model of a flat earth, the direct signal is given by [26]

$$x_d(t) = x(t)e^{-j\kappa R_d} \tag{2}$$

the indirect signal is

$$x_i(t) = x(t)\rho e^{j\phi}e^{-j\kappa R_i} \tag{3}$$

where $\rho e^{j\phi}$ is the complex reflection coefficient, $\kappa = 2\pi/\lambda$ the wave number, and R_i the total length of the indirect path. The target range

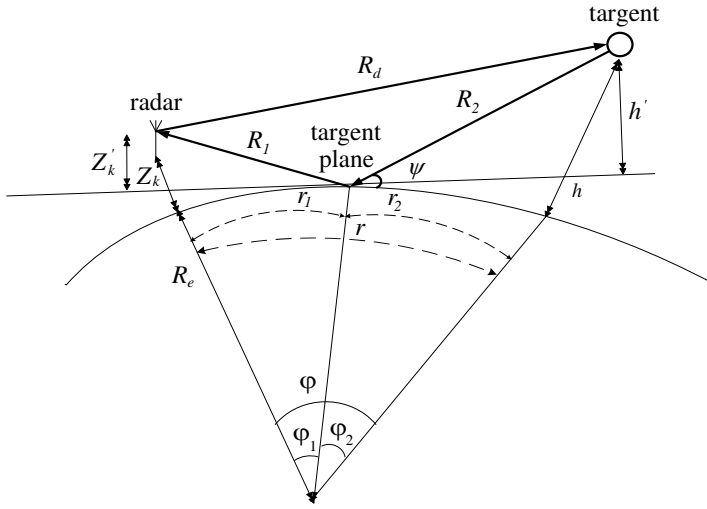

Figure 1. Multipath geometry for a curved earth.

R_d can be obtained from the time delay. Thus, the total received signal is given by

$$x_r(t) = x_d(t) + x_i(t) \tag{4}$$

To model the received signals more accurately, the curvature of the signal path due to refraction in the troposphere, in addition to the curvature of the earth itself, must be taken into account. The multipath geometry for a curved earth is given in Fig. 1.

Firstly, obtain φ according to the law of cosine as

$$\varphi = \arccos\left(\frac{(h+R_e)^2 + (\mathrm{Z}_k + R_e)^2 - R_d^2}{2\,(h+R_e)\,(\mathrm{Z}_k + R_e)}\right) \tag{5}$$

where, $\arccos(\cdot)$ stands for the arccosine, and h and Z_k are the height of target and height of radar, respectively. R_e is the effective radius of the imaginary earth, given by

$$R_e = R_0\left(1 + 6.37 \times 10^{-3}\frac{dU}{dh}\right)^{-1} \tag{6}$$

where U is called the radio refractivity.

The horizon distance is computed by $r = R_e\varphi$, and the distance from the radar to the point of reflection r_1 can be found by solving the following cubic equation as [27]

$$2r_1^3 - 3rr_1^2 + \Big[r^2 - 2R_e(Z_k + h)\Big]r_1 + 2R_eZ_kr = 0 \tag{7}$$

Next, we solve φ_1, φ_2 using r_1 by

$$\varphi_1 = r_1/R_e \tag{8}$$

$$\varphi_2 = (r - r_1)/R_e \tag{9}$$

using the law of cosine yields

$$R_1 = \sqrt{R_e^2 + (R_e + Z_k)^2 - 2R_e(R_e + Z_k)\cos\varphi_1} \tag{10}$$

$$R_2 = \sqrt{R_e^2 + (R_e + h)^2 - 2R_e(R_e + h)\cos\varphi_2} \tag{11}$$

$$R_d = \sqrt{(h + R_e)^2 + (R_e + Z_k)^2 - 2(h + R_e)(R_e + Z_k)\cos(\varphi_1 + \varphi_2)} \tag{12}$$

then, the grazing angle ψ is

$$\psi = \frac{\pi}{2} - \frac{1}{2}\arcsin\left(\frac{R_1^2 + R_2^2 - R_d^2}{2R_1R_2}\right) \tag{13}$$

The term $\rho e^{j\phi}$ in (3) generally consists of the Fresenl reflection coefficient, divided into the vertical polarization Γ_v and horizontal polarization Γ_h, the divergence factor D due to a curved surface, and the surface roughness factor ρ_s, i.e., $\rho e^{j\phi} = \Gamma_{(v,h)} D \rho_s$. The vertical polarization and horizontal polarization Fresnel reflection coefficients are respectively [26]

$$\Gamma_v \simeq \frac{\psi\sqrt{\varepsilon_c} - 1}{\psi\sqrt{\varepsilon_c} + 1} \tag{14}$$

$$\Gamma_h \simeq \frac{\psi - \sqrt{\varepsilon_c}}{\psi + \sqrt{\varepsilon_c}} \tag{15}$$

where ψ is the grazing angle and ε_c is the complex dielectric constant which is given by

$$\varepsilon_c = \varepsilon/\varepsilon_0 - j60\lambda\sigma \tag{16}$$

$\varepsilon/\varepsilon_0$ is the relative dielectric constant of the reflecting medium, and σ is its conductivity. Thus, the Fresnel reflection coefficient is determined by the grazing angle under a deterministic condition.

When an electromagnetic wave is incident on a round earth surface, the reflected wave diverges because of the earth's curvature. Then, the reflected energy is defocused and radar power density is reduced. The divergence factor can be derived solely from geometrical considerations. A widely accepted approximation for the divergence factor D is given by [26]

$$D \simeq \left(1 + \frac{2r_1r_2}{R_e r\psi}\right)^{-1/2} \tag{17}$$

The surface roughness factor ρ_s is given by

$$\rho_s = e^{-\mu} \tag{18}$$

$$\mu = \begin{cases} 2\left[2\pi\eta\right]^2 & \eta \leq 0.1\,\text{rad} \\ 0.16\eta^2 + 7.42\eta + 0.0468 & \text{otherwise} \end{cases} \tag{19}$$

and η is the surface roughness factor given by

$$\eta = \frac{\sigma_H \psi}{\lambda} \tag{20}$$

and σ_H is the Root-Mean-Square (RMS) surface height irregularity. For simplicity, the diffuse component is treated as the incoherent white Gaussian noise. From (13)–(19), we can see that the specular reflection coefficient depends on the grazing angle. The other parameters can be obtained when a model is given, therefore, the specular reflection coefficient is a function of the grazing angle ψ, i.e., $f(\psi) = \rho e^{j\phi}$. Submitting (13)–(19) in $f(\psi) = \rho e^{j\phi}$ yields

$$\rho e^{j\phi} = \left(\frac{a_1 + b_1}{c_1} + j\frac{a_2 - b_2}{c_1}\right) \times \left(1 + \frac{2r_1 r_2}{R_e r \psi}\right)^{-1/2} e^{-\mu} \tag{21}$$

where

$$\begin{cases} a_1 = \left(\psi^2 k \cos\theta - 2\psi k^{\frac{1}{2}} \cos\dfrac{\theta}{2} + 1\right)\left(\psi^2 k \cos\theta - 1\right) \\ b_1 = \left(\psi^2 k \sin\theta - \psi k^{\frac{1}{2}} \sin\dfrac{\theta}{2}\right)\psi^2 k \sin\theta \\ a_2 = \psi^2 k \sin\theta \left(\psi^2 k \cos\theta - 2\psi k^{\frac{1}{2}} \cos\dfrac{\theta}{2} + 1\right) \\ b_2 = \left(\psi^2 k \cos\theta - 1\right)\left(\psi^2 k \sin\theta - \psi k^{\frac{1}{2}} \sin\dfrac{\theta}{2}\right) \\ c_1 = \left(\psi^2 k \cos\theta - 1\right)^2 + \psi^4 k^2 \sin^2\theta \\ k = \sqrt{\left(\dfrac{\varepsilon}{\varepsilon_0}\right)^2 + (60\lambda\sigma)^2} \\ \theta = \arctan\dfrac{\varepsilon}{60\lambda\sigma\varepsilon_0} \end{cases} \tag{22}$$

thus, ρ is given by

$$\rho = \sqrt{\left(\frac{a_1 + b_1}{c_1}\right)^2 + \left(\frac{a_2 - b_2}{c_1}\right)^2} DS \tag{23}$$

3. SYSTEMS DESIGN CRITERION

In this section, we will introduce the multipath signal model of MIMO radar and phased-array radar, respectively.

3.1. MIMO Radar

3.1.1. Multipath Geometry Model for MIMO radar

Assume that there are M transmitters and N receivers in MIMO radar system. The baseband received signal model of MIMO radar is [14]

$$\mathbf{r}(t) = \sqrt{\frac{E}{M}}\mathrm{diag}(\mathbf{a})\,\mathbf{H}\mathrm{diag}(\mathbf{b})\,\mathbf{s}(t-\tau) + \mathbf{n}(t) \tag{24}$$

where E is the total received signal energy of all receivers; $\mathbf{a} = [1, e^{j\phi_{r2}}, \ldots, e^{j\phi_{rN}}]^T$ is an $N \times 1$ receiving steering vector; ϕ_{rn} is the phase difference between the nth receiver and the first receiver; $\mathbf{b} = [1, e^{j\phi_{t2}}, \ldots, e^{j\phi_{tM}}]^T$ is an $M \times 1$ transmitting steering vector; ϕ_{tm} is the phase difference between the mth transmitter and first transmitter; the elements of $\mathbf{H}$ are zero-mean, unit variance complex normal random variable. Denote by $\boldsymbol{\alpha} = [\alpha_{11}, \ldots, \alpha_{1M}, \alpha_{21}, \ldots, \alpha_{NM}]^T$ the vector that contains all the elements of the matrix $\mathbf{H}$, $\mathbf{n}(t) = [n_1(t), n_2(t), \ldots, n_N(t)]^T$ is a white, zero-mean, complex normal random process with correlation matrix $\sigma_n^2\mathbf{I}_N$.

3.1.2. Multipath Signal Model of MIMO Radar

In the presence of multipath, considering atmosphere refraction and the curved earth effect, the reflected signals from a point target of MIMO radar include four parts: directly-directly path, directly-reflected path, reflected-directly path, reflected-reflected path. Assume the point target located at $X_0 = (x_0, y_0)$ and reflected point in ground located at $X_i = (x_i, y_i)$, $i = 1, 2$. Fig. 2 illustrates a four-way MIMO radar propagation model with multipath.

The directly-directly path echo signal is given by (24). When the height of target is less than a beamwidth, the difference delay of multipath will be very small [16]. The directly-reflected path echo signal is

$$\mathbf{r}^{(dr)}(t) = \sqrt{\frac{E}{M}}\mathrm{diag}(\mathbf{a})\,\mathbf{K}^{(dr)}\mathbf{H}\mathrm{diag}(\mathbf{b})\,\mathbf{s}(t-\tau) + \mathbf{n}(t) \tag{25}$$

where $\mathbf{K}^{(dr)} = \begin{bmatrix} \rho_{11}^{(dr)} & \cdots & \rho_{1M}^{(dr)} \\ \vdots & \ddots & \vdots \\ \rho_{N1}^{(dr)} & \cdots & \rho_{NM}^{(dr)} \end{bmatrix}$ and $\rho_{kj}^{(dr)}$ is the amplitude of reflect

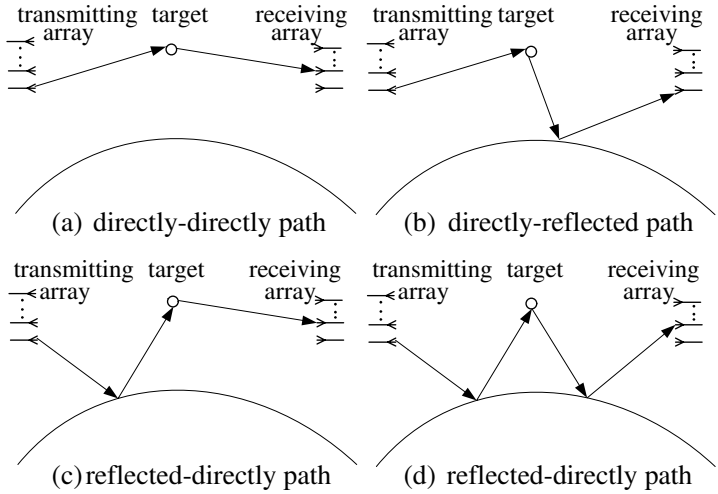

Figure 2. Four received signal components of MIMO radar with multipath.

coefficient, τ is the time delay given by

$$\begin{aligned}\tau &= \tau_{tk}(X_0) + \tau_{rl}(X_0) \\ &= \frac{\sqrt{(x_{tk}-x_0)^2+(y_{tk}-y_0)^2}}{c} + \frac{\sqrt{(x_{rl}-x_0)^2+(y_{rl}-y_0)^2}}{c} \quad (26)\end{aligned}$$

The reflected-directly path echo signal is

$$\mathbf{r}^{(rd)}(t) = \sqrt{\frac{E}{M}}\mathrm{diag}(\mathbf{a})\,\mathbf{K}^{(rd)}\mathbf{H}\mathrm{diag}(\mathbf{b})\,s(t-\tau) + \mathbf{n}(t) \quad (27)$$

The reflected-reflected path echo signal is

$$\mathbf{r}^{(rr)}(t) = \sqrt{\frac{E}{M}}\mathrm{diag}(\mathbf{a})\,\mathbf{K}^{(rr)}\mathbf{H}\mathrm{diag}(\mathbf{b})\,s(t-\tau) + \mathbf{n}(t) \quad (28)$$

Thus, the received signal of MIMO radar with multipath is

$$\begin{aligned}\mathbf{r}(t) &= \mathbf{r}^{(dd)}(t) + \mathbf{r}^{(dr)}(t) + \mathbf{r}^{(rd)}(t) + \mathbf{r}^{(rr)}(t) \\ &= \sqrt{\frac{E}{M}}\mathrm{diag}(\mathbf{a})\,\mathbf{K}\odot\mathbf{H}\mathrm{diag}(\mathbf{b})\,\mathbf{s}(t-\tau) + \mathbf{n}(t) \quad (29)\end{aligned}$$

where

$$\begin{aligned}\mathbf{K} &= \mathbf{I} + \mathbf{K}^{(dr)} + \mathbf{K}^{(rd)} + \mathbf{K}^{(rr)} \\ &= \begin{bmatrix} 1+\rho_{11}^{(dr)}+\rho_{11}^{(rd)}+\rho_{11}^{(rr)} & \cdots & 1+\rho_{1M}^{(dr)}+\rho_{1M}^{(rd)}+\rho_{1M}^{(rr)} \\ \vdots & \ddots & \vdots \\ 1+\rho_{N1}^{(dr)}+\rho_{N1}^{(rd)}+\rho_{N1}^{(rr)} & \cdots & 1+\rho_{NM}^{(dr)}+\rho_{NM}^{(rd)}+\rho_{NM}^{(rr)} \end{bmatrix}\end{aligned}$$

and $\mathbf{I}$ is the identity matrix. Let $K_{ij} = 1 + \rho_{ij}^{(dr)} + \rho_{ij}^{(rd)} + \rho_{ij}^{(rr)}$ and $\mathbf{H}' = \mathbf{K} \odot \mathbf{H}$, (29) can be expressed as

$$\mathbf{r}(t) = \sqrt{\frac{E}{M}} \mathrm{diag}(\mathbf{a}) \mathbf{H}' \mathrm{diag}(\mathbf{b}) s(t-\tau) + \mathbf{n}(t) \tag{30}$$

and $\mathbf{H}'_{ij} = k_{ij}\alpha_{ij} \sim \mathcal{CN}(0, k_{ij}^2)$.

3.2. Phased-array Radar

3.2.1. Multipath Geometry Model for Phased-array Radar

For the traditional phased-array radar systems which utilize an array of closely spaced sensors, their received signal model is given by [14]:

$$r(t) = \sqrt{\frac{E}{M}} \alpha \tilde{\mathbf{a}}^H \mathbf{a} \mathbf{b}^H \tilde{\mathbf{b}} s(t-\tau) + n(t) \tag{31}$$

where $\tilde{\mathbf{b}}$ is usually referred to as the transmitter steering vector, and $\tilde{\mathbf{a}}$ is the receiver steering vector. $n(t)$ is a zero-mean complex normal random process with variance $N\sigma_n^2$. To increase SNR, and $\tilde{\mathbf{a}}$ and $\tilde{\mathbf{b}}$ are usually chosen such that $\tilde{\mathbf{a}}^H \mathbf{a} = N$ and $\mathbf{b}^H \tilde{\mathbf{b}} = M$.

3.2.2. Multipath Signal Model of Phased-array Radar

In the presence of multipath, the reflected radar signals from a point target of phased-array radar also include four parts: directly-directly path, directly-reflected path, reflected-directly path and reflected-reflected path. The directly-directly path echo signal is given by (31), the directly-reflected path echo signal is

$$r_{Phased}^{(dr)}(t) = \sqrt{\frac{E}{M}} \rho^{(dr)} \alpha \tilde{\mathbf{a}}^H \mathbf{a} \mathbf{b}^H \tilde{\mathbf{b}} s(t-\tau) + n(t) \tag{32}$$

The reflected-directly path echo signal is

$$r_{Phased}^{(rd)}(t) = \sqrt{\frac{E}{M}} \rho^{(rd)} \alpha \tilde{\mathbf{a}}^H \mathbf{a} \mathbf{b}^H \tilde{\mathbf{b}} s(t-\tau) + n(t) \tag{33}$$

The reflected-reflected path echo signal is

$$r_{Phased}^{(rr)}(t) = \sqrt{\frac{E}{M}} \rho^{(rr)} \alpha \tilde{\mathbf{a}}^H \mathbf{a} \mathbf{b}^H \tilde{\mathbf{b}} s(t-\tau) + n(t) \tag{34}$$

where $\rho^{(dr)} = \rho^{(rd)}$ and $\rho^{(rr)} = \rho^{(rd)} \times \rho^{(dr)}$. Thus, the received signal of phase-array radar in multipath is

$$r_{Phased}(t) = \sqrt{\frac{E}{M}} \left(1 + \rho^{(dr)}\right)^2 \alpha \tilde{\mathbf{a}}^H \mathbf{a} \mathbf{b}^H \tilde{\mathbf{b}} s(t-\tau) + n(t) \tag{35}$$

4. LOW-GRAZING ANGLE DETECTOR OF MIMO RADAR

4.1. MIMO Radar

We formulate the MIMO radar detection problem. The binary hypothesis test for MIMO is

$$\begin{cases} H_0: \text{ target absence} \\ H_1: \text{ target presence} \end{cases} \tag{36}$$

Assume that $\boldsymbol{\alpha}$ is an $NM \times 1$ vector. Let $\boldsymbol{\beta} = \boldsymbol{\alpha} \odot \mathbf{k}$. Denote $\mathbf{x}$ the $NM \times 1$ vector and the element of which is $[\mathbf{x}]_{iN+j} \stackrel{\Delta}{=} \int r_i(t) s_j(t-\tau) dt$, i.e., $\mathbf{x}$ is the output of a bank of matched filters. The Probability Density Function (PDF) of the received measurements under both the alternative and null hypotheses are respectively given by

$$\begin{aligned} f(\mathbf{r}(t)|H_1) &= \int f(\mathbf{r}(t)|H_1, \boldsymbol{\beta}) f(\boldsymbol{\beta}) d\boldsymbol{\beta} \\ &= \int ce^{-\frac{1}{\sigma_n^2}\int \left\|\mathbf{r}(t)-\mathbf{H}'\sqrt{\frac{E}{M}}s(t-\tau)\right\|^2 dt} f(\boldsymbol{\beta}) d\boldsymbol{\beta} \\ &= \int ce^{-\frac{1}{\sigma_n^2}\sum_i \int \left|r_i(t)-\sqrt{\frac{E}{M}}\sum_{j=1}^M \beta_{ij} s_j(t)\right|^2 dt} f(\boldsymbol{\beta}) d\boldsymbol{\beta} \\ &= \int ce^{-\frac{1}{\sigma_n^2}\sum_i \int |r_i(t)|^2 dt - \sqrt{\frac{E}{M}}\sum_{j=1}^M \beta_{ij}^* \int r(t) s_j^*(t-\tau) dt - \sqrt{\frac{E}{M}}} \\ &\quad \cdot \sum_{j=1}^M \beta_{ij} \int r^*(t) s_j(t-\tau) + \frac{E}{M}\sum_{j=1}^M |\beta_{ij}|^2 f(\boldsymbol{\beta}) d\boldsymbol{\beta} \\ &= c' e^{-\frac{\int \|\mathbf{r}(t)\|^2 dt}{\sigma_n^2}} \int e^{-\frac{1}{\sigma_n^2}\left(-\sqrt{\frac{E}{M}}\boldsymbol{\beta}^H\mathbf{x} - \sqrt{\frac{E}{M}}\mathbf{x}^H\boldsymbol{\beta} + \left\|\sqrt{\frac{E}{M}}\boldsymbol{\beta}\right\|^2\right)} e^{-\|\boldsymbol{\beta}\|^2} d\boldsymbol{\beta} \\ &= c' e^{-\frac{\int \|\mathbf{r}(t)\|^2 dt}{\sigma_n^2} + \frac{\frac{E}{M}\|\mathbf{x}\|^2}{\sigma_n^2\left(\sigma_n^2+\frac{E}{M}\right)}} \int e^{-\frac{1}{\sigma_n^2}\left\|\sqrt{\sigma_n^2+\frac{E}{M}}\boldsymbol{\beta} - \frac{\sqrt{\frac{E}{M}}\mathbf{x}}{\sqrt{\sigma_n^2+\frac{E}{M}}}\right\|^2} d\boldsymbol{\beta} \\ &= c'' e^{-\frac{\int \|\mathbf{r}(t)\|^2 dt}{\sigma_n^2} + \frac{\frac{E}{M}\|\mathbf{x}\|^2}{\sigma_n^2\left(\sigma_n^2+\frac{E}{M}\right)}} \end{aligned} \tag{37}$$

$$f(\mathbf{r}(t)|H_0) = ce^{-\frac{\int \|\mathbf{r}(t)\|^2 dt}{\sigma_n^2}} \tag{38}$$

where $c = \frac{1}{\sqrt{2\pi}\sigma_n}$, $c' = c\frac{1}{\sqrt{2\pi \sum_{i=1}^{N}\sum_{j=1}^{M} k_{kj}^2}} e^{-\frac{1}{2\sum_{i=1}^{N}\sum_{j=1}^{M} k_{kj}^2}}$, and $c'' = c' \int e^{-\frac{1}{\sigma_n^2}\left\|\sqrt{\sigma_n^2+\frac{E}{M}}\boldsymbol{\beta}-\frac{\sqrt{\frac{E}{M}}\mathbf{x}}{\sqrt{\sigma_n^2+\frac{E}{M}}}\right\|^2} d\boldsymbol{\beta}$.

Thus, the low-grazing angle likelihood ratio test (LRT) detector for MIMO radar systems is given by

$$Y = \log \frac{f\left(\mathbf{r}\left(t\right)|H_1\right)}{f\left(\mathbf{r}\left(t\right)|H_0\right)} = \frac{\frac{E}{M}\left\|\mathbf{x}\right\|^2}{\sigma_n^2\left(\sigma_n^2+\frac{E}{M}\right)} \log\frac{c''}{c} \begin{array}{l} > H_1 \\ < H_0 \end{array} T \tag{39}$$

(39) can be simplified as

$$Y = \left\|\mathbf{x}\right\|^2 \begin{array}{l} > H_1 \\ < H_0 \end{array} \delta \tag{40}$$

where $\delta = \frac{T\sigma_n^2(\sigma_n^2+\frac{E}{M})}{\frac{E}{M}}$, δ is a threshold.

It is easy to verify that $\mathbf{x}$ is distributed as follows:

$$\mathbf{x} = \begin{cases} \mathbf{n} & H_0 \\ \sqrt{\dfrac{E}{M}}\boldsymbol{\beta} + \mathbf{n} & H_1 \end{cases} \tag{41}$$

where $\mathbf{n} \sim \mathcal{CN}(0, \sigma_n^2\mathbf{I}_{MN})$ and $\beta_{ij} \sim \mathcal{CN}(0, k_{ij}^2\mathbf{I}_{MN})$. Therefore, $\mathbf{x}$ is a zero-mean complex random variable with correlation matrix $\sigma_n^2\mathbf{I}_{MN}$ under the null hypothesis, and $((E/M)k_{ij}^2 + \sigma_n^2)\mathbf{I}_{MN}$ under the alternate hypothesis. The test statistic distributed as follows:

$$\left\|\mathbf{x}\right\|^2 \sim \begin{cases} \dfrac{\sigma_n^2}{2}\chi_{(2MN)}^2 & H_0 \\ \chi_{(2)}^2 \displaystyle\sum_{i=1}^{N}\sum_{j=1}^{M}\left(\frac{E}{2M}k_{ij}^2 + \frac{\sigma_n^2}{2}\right) & H_1 \end{cases} \tag{42}$$

where $\chi_{(d)}^2$ denotes a chi-square random variable with d degrees of freedom.

The probability of false alarm can be expressed as

$$P_{FA} = P\left(Y > \delta|H_0\right) = P\left(\frac{\sigma_n^2}{2}\chi_{(2MN)}^2 > \delta\right) = P\left(\chi_{(2MN)}^2 > \frac{2\delta}{\sigma_n^2}\right) \tag{43}$$

It follows that δ is set using the following formula:

$$\delta = \frac{\sigma_n^2}{2} F_{\chi_{(2MN)}^2}^{-1}\left(1 - P_{FA}\right) \tag{44}$$

where $F^{-1}_{\chi^2_{(2MN)}}$ denotes the inverse cumulative distribution function of a chi-square random variable with $2MN$ degrees of freedom. The probability of detection is given by

$$P_D = P\left(Y > \delta | H_1\right) = P\left(\left(\frac{\sigma_n^2}{2} + \frac{E}{2M}\sum_{i=1}^{N}\sum_{j=1}^{M} k_{ij}^2\right)\chi^2_{(2)} > \delta\right)$$
$$= 1 - F_{\chi^2_{(2)}}\left(\frac{2\delta}{\sigma_n^2 + \frac{E}{M}\sum\limits_{i=1}^{N}\sum\limits_{j=1}^{M} k_{ij}^2}\right) \tag{45}$$

4.2. Phased-array Radar

Consider a phased-array radar system. Let $x = \int \mathbf{r}^H(t)\mathbf{a}s(t-\tau)dt$ be the output of the spatial-temporal matched filter and assume $\ell = (1+\rho^{(dr)})^2\alpha$. The PDF of phased-array radar under the alternative hypotheses is given by

$$f(\mathbf{r}(t)|H_1) = f(\mathbf{r}(t)|H_1,\ell)f(\mathbf{l})d\mathbf{l} = \int ce^{-\frac{1}{\sigma_n^2}\int\left\|\mathbf{r}(t)-\sqrt{\frac{E}{M}}\ell\mathbf{a}\mathbf{b}^H\tilde{\mathbf{b}}s(t-\tau)\right\|dt} f(\ell)d\ell$$
$$= ce^{-\frac{\int\|r(t)\|^2dt}{\sigma_n^2}} \int e^{-\frac{1}{\sigma_n^2}\left(-2\sqrt{\frac{E}{M}}\Re\left(\ell\mathbf{b}^H\tilde{\mathbf{b}}\int \mathrm{r}^H(t)\mathbf{a}s(t-\tau)dt\right)+\frac{E}{M}|\ell|^2\left\|\tilde{\mathbf{b}}^H\mathbf{b}\mathbf{a}\right\|^2\right)+|\ell|^2 d\ell}$$
$$= c'e^{-\frac{\int\|r(t)\|^2dt}{\sigma_n^2} - \frac{E|\mathbf{b}\tilde{\mathbf{b}}|^2|x|^2}{M\sigma_n^2\left(1+\frac{E}{M}|\mathbf{b}\tilde{\mathbf{b}}|^2\right)}} \tag{46}$$

the PDF under null hypotheses is the same as in (38).

Thus, the low-grazing angle LRT detector for phased-array radar systems is given by

$$Y' = \log\frac{f\left(\mathrm{r}\left(t\right)|H_1\right)}{f\left(\mathrm{r}\left(t\right)|H_0\right)} = \frac{E\left|\mathrm{b}\tilde{\mathrm{b}}\right|^2|x|^2}{M\sigma_n^2\left(1+\frac{E}{M}\left|b\tilde{b}\right|^2\right)} \log\frac{c'}{c} \begin{array}{l} > H_1 \\ < H_0 \end{array} T' \tag{47}$$

It is easy to verify that x is satisfied as

$$x = \begin{cases} n & H_0 \\ \sqrt{\dfrac{E}{M}}N^2M^2\left(1+\rho^{(dr)}\right)^2\alpha + n & H_1 \end{cases} \tag{48}$$

This gives rise to the following distribution of the test statistic:

$$Y' = \begin{cases} \dfrac{\sigma_n^2 N}{2}\chi^2_{(2)} & H_0 \\ \left(\dfrac{\sigma_n^2 N}{2} + \dfrac{EN^2M^2\left(1+\rho^{(dr)}\right)^2}{2M}\right)\chi^2_{(2)} & H_1 \end{cases} \tag{49}$$

The probability of false alarm, the probability of detection, and the threshold are, respectively, given by

$$P_{FA} = P\left(\chi^2_{(2)} > \frac{2\delta}{N\sigma_n^2}\right) \tag{50}$$

$$\delta = \frac{N\sigma_n^2}{2}F^{-1}_{\chi^2_{(2)}}\left(1-P_{FA}\right) \tag{51}$$

$$P_D = 1 - F_{\chi^2_{(2)}}\left(\frac{1}{1+\frac{E}{\sigma_n^2}NM\left(1+\rho^{(dr)}\right)^2}F^{-1}_{\chi^2_{(2)}}\left(1-P_{FA}\right)\right) \tag{52}$$

5. SYSTEM CONFIGURATION OF MIMO RADAR

In [14], the deflection coefficient, called "detectors SNR", is adopted to describe the detection performance of MIMO radar system. The expressions of deflection coefficient is

$$\beta_{dc} = \frac{\left|E\left(Y|H_0\right) - E\left(Y|H_1\right)\right|^2}{1/2\left[\mathrm{var}\left(Y|H_0\right) + \mathrm{var}\left(Y|H_1\right)\right]} \tag{53}$$

where $E(Y|H_t)$, $t = 0, 1$, are the means of detector's test under the null and alternate, and $\mathrm{var}(Y|H_t)$, $t = 0, 1$ are the variances of detector's test under the null and alternate. In this paper, we will use the deflection coefficient as the criterion of the configuration design both for MIMO radar systems and phased-array radar.

Let $k_m = \sum_{i=1}^{N}\sum_{j=1}^{M} k_{ij}^2$. According to (42), $E(Y|H_0) = MN\sigma_n^2$, and $E(Y|H_1) = \frac{E}{M}k_m + \sigma_n^2$, hence $|E(Y|H_0) - E(Y|H_1)|^2 = [(MN-1)\sigma_n^2 - \frac{E}{M}k_m]^2$. Also, according to (42), $\mathrm{var}(Y|H_0) = MN\sigma_n^4$, and $\mathrm{var}(Y|H_1) = \frac{E^2}{M^2}k_m^2 + 2E\sigma_n^2 + \sigma_n^4$, hence, $[\mathrm{var}(Y|H_0) + \mathrm{var}(Y|H_1)] = \frac{E^2}{M^2}k_m^2 + 2E\sigma_n^2 k_m + \sigma_n^4(MN+1)$. Combining these results, the SNR of the detector of MIMO radar is given by

$$\beta_{dc} = \frac{\left[\left(MN-1\right)\sigma_n^2 - \frac{E}{M}k_m\right]^2}{\frac{E^2}{M^2}k_m^2 + 2E\sigma_n^2 k_m + \sigma_n^4\left(MN+1\right)} \tag{54}$$

We define the SNR as $\rho \triangleq \frac{E}{\sigma_n^2}$, which is the ratio of the total signal energy to the noise level at each receiver. Thus (54) can be simplified into

$$\beta_{dc} = \frac{2M^2 (MN-1)^2 - 4M (MN-1) \rho k_m + 2\rho^2 k_m^2}{\rho^2 k_m^2 + 2M\rho k_m + M^2 (MN+1)} \tag{55}$$

For MIMO radar system, the optimization configuration problem is

$$\begin{aligned} &\max_{M,N} \beta_{dc} = \frac{2M^2 (MN-1)^2 - 4M (MN-1) \rho^2 k_m + 2\rho^2 k_m^2}{2\rho^2 k_m^2 + 2M^2 \rho k_m + M^2 (MN+1)} \\ &s.t. \;\; M + N = L \end{aligned} \tag{56}$$

Using Lagrange method, we have the following optimization function:

$$F(M,N) = \beta_{dc} + \gamma (M + N - L) \tag{57}$$

and define

$$\begin{aligned} u &= 2M^2 (MN-1)^2 - 4M (MN-1) \rho^2 k_m + 2\rho^2 k_m^2 \\ v &= 2\rho^2 k_m^2 + 2M^2 \rho k_m + M^2 (MN+1) \\ A &= 8M^3 N^2 - 12M^2 N + 4M - 8\rho MN k_m + 4\rho k_m \\ B &= 3M^2 N + 2M + 2\rho k_m \end{aligned} \tag{58}$$

take derivation to M and let the result be equal to zero

$$\frac{\partial F(M,N)}{\partial M} = \frac{Av - uB}{\left[M^2 (MN+1) + 2M^2 \rho k_m + 2\rho^2 k_m^2\right]^2} + \gamma = 0 \tag{59}$$

Similarly, take derivative to N and let the result be equal to zero. Then we have

$$\frac{\partial F}{\partial N} = \frac{\left(4M^4 N - 4M^3 - 4\rho M^2 k_m\right) v - uM^3}{\left[M^2 (MN+1) + 2M\rho k_m + 2\rho^2 k_m^2\right]^2} + \gamma = 0 \tag{60}$$

comparing (59) with (60), we have

$$\begin{aligned} A &= 4M^4 N - 4M^3 - 4\rho M^2 k_m \\ 3M^2 N + 2M + 2\rho k_m &= M^3 \end{aligned} \tag{61}$$

It is difficult to get an analytical result of this problem.

Now we analyze the deflection coefficient of phased-array radar. According to (49), $E(Y'|H_0) = N\sigma_n^2$, and $E(Y'|H_1) = N\sigma_n^2 + EN^2 M(1+\rho^{(dr)})^2$, then, $|E[Y'|H_0] - E[Y'|H_1]|^2 = E^2 N^4 M^2 (1+\rho^{(dr)})^4$. Also, according to (49), $\mathrm{var}(Y'|H_0) = N^2\sigma_n^4$, and $\mathrm{var}(Y'|H_1) = [EN^2 M(1+\rho^{(dr)})^2 + N\sigma_n^2]^2$, hence, $\mathrm{var}(Y'|H_0) + \mathrm{var}(Y'|H_1) =$

$2N^2\sigma_n^4 + 2EN^3M\sigma_n^2(1+\rho^{(dr)})^2 + E^2N^4M^2(1+\rho^{(dr)})^4$. Combining these results, the detector SNR of phased-array radar is given by

$$\beta_{dc\_Phase} = \frac{\rho^2N^2M^2\left(1+\rho^{(dr)}\right)^4}{1+\rho NM\left(1+\rho^{(dr)}\right)^2+\rho^2N^2M^2\left(1+\rho^{(dr)}\right)^4\Big/2} \tag{62}$$

Using Lagrange method, we have the following optimization function:

$$F_{Phase}(M,N) = \beta_{dc\_Phase} + \gamma(M+N-L) \tag{63}$$

For phased-array radar system, the optimization problem is

$$\begin{aligned} &\max_{M,N}\beta_{dc\_Phase} = \frac{\rho^2N^2M^2\left(1+\rho^{(dr)}\right)^4}{1+\rho NM\left(1+\rho^{(dr)}\right)^2+\rho^2N^2M^2\left(1+\rho^{(dr)}\right)^4\Big/2} \\ &s.t. \qquad M+N=L \end{aligned} \tag{64}$$

and define

$$\begin{aligned} u' &= \rho^2N^2M^2\left(1+\rho^{(dr)}\right)^4 \\ v' &= 1+\rho NM\left(1+\rho^{(dr)}\right)^2+\rho^2N^2M^2\left(1+\rho^{(dr)}\right)^4\Big/2 \\ A' &= 2\rho^2N^2M\left(1+\rho^{(dr)}\right)^4 \\ B' &= \rho N\left(1+\rho^{(dr)}\right)^2+\rho^2N^2M\left(1+\rho^{(dr)}\right)^4 \\ C' &= 1+\rho NM\left(1+\rho^{(dr)}\right)^2+\rho^2N^2M^2\left(1+\rho^{(dr)}\right)^4\Big/2 \\ D' &= 2\rho^2M^2N\left(1+\rho^{(dr)}\right)^4 \\ E' &= \rho M\left(1+\rho^{(dr)}\right)^2+\rho^2NM^2\left(1+\rho^{(dr)}\right)^4 \end{aligned} \tag{65}$$

take derivation to M and let the result be equal to zero

$$\frac{\partial F_{Phase}}{\partial M} = \frac{A'v'-u'B'}{(C')^2} + \gamma = 0 \tag{66}$$

Similarly, take derivative to N and let the result be equal to zero. Then we have

$$\frac{\partial F_{Phase}}{\partial N} = \frac{D'v'-u'E'}{(C')^2} + \gamma = 0 \tag{67}$$

comparing (66) with (67), we have $M = N$. Therefore, for a phased-array radar, the optimal configuration is obtained when $M = N$.

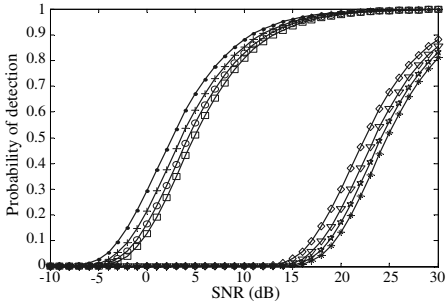

Figure 3. MIMO radar low-grazing angle detection performance, $P_{FA} = 10^{-5}$ multipath ($\bullet$ curve), $P_{FA} = 10^{-6}$ multipath ($+$ curve), $P_{FA} = 10^{-7}$ multipath ($\circ$ curve), $P_{FA} = 10^{-8}$ multipath ($\square$ curve), $P_{FA} = 10^{-5}$ non-multipath ($\Diamond$ curve), $P_{FA} = 10^{-6}$ non-multipath (∇ curve), $P_{FA} = 10^{-7}$ non-multipath ($\star$ curve), $P_{FA} = 10^{-8}$ non-multipath ($*$ curve).

6. NUMERICAL SIMULATIONS

In this section, we consider several numerical examples to illustrate our analytical results. In our first example, we consider four-transmit-antenna and four-receive-antenna systems. The heights of transmit array are fixed at 10 m, 80 m, 200 m, 300 m, respectively, the heights of receive antennas fixed at 100 m, 200 m, 300 m, 400 m, respectively, and the target's height fixed at fixed at 500 m. First, we consider the performance of the detection for MIMO radar in different probability of false alarm. Fig. 3 depicts the probability of detection of the optimal detectors considering with multipath effects and without multipath effect, respectively, as a function of the SNR. The probabilities of false alarm are fixed at $\mathrm{P}_{FA} = 10^{-5}$, 10^{-6}, $10^{-7}, 10^{-8}$, respectively.

For the same SNR and false alarm, the performance of detector with multipath outperforms the detector without considering multipath effect, the SNR can be improved by employed the multipath effect. Under the same probability of detection, the detectors without multipath need much greater SNR. Therefore, when we detect a target in low-grazing angle, the multipath effects must be considered and utilized.

Figure 4 depicts the optimal detectors' SNR both for the phased-array and MIMO systems. We assume $M = N = 4$ and that the noise level is constant across the array. It is evident from the figures that, MIMO radar systems have better performance than the phased-array radar. This figure establishes the advantage of the MIMO radar system

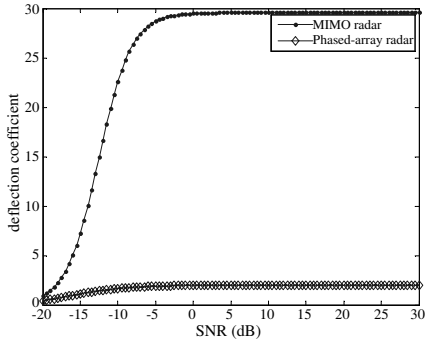

Figure 4. Optimal detector's SNR both for MIMO radar and phased-array radar.

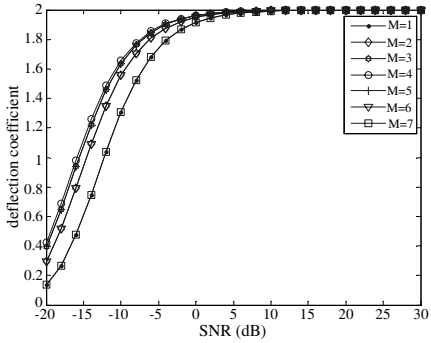

Figure 5. Performance of different schemes for phased-array radar.

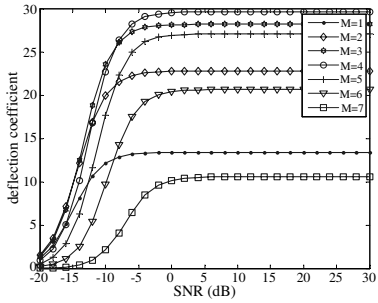

Figure 6. Performance of different schemes for MIMO radar.

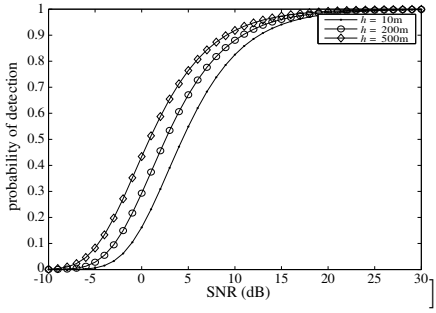

Figure 7. Performance varies with the height of target.

over the phased-array radar system.

Figure 5 depicts the optimal configuration of phased-array radar. When $L = 8$ and M is increased from 1 to 7. Fig. 5 shows that when $M = 4$, the best performance is achieved, which agrees with the analytical results in Section 6 and the conclusion in [21].

Figure 6 depicts the optimal configuration of MIMO radar. When the SNR is greater than -10 dB and the number of transmitter equal to that of the receiver, the system has the best detection performance. When the SNR is less than -10 dB, the case of $M = 3$ provides the best performance, and the results are different from literature [25], which result from the different considered scenes, i.e., with or without multipath environment.

In Fig. 7, the heights of target are fixed at 10 m, 200 m, 500 m and the probabilities of false alarm fixed at $\mathrm{P}_{FA} = 10^{-5}$. The figure shows

that the detection performance varies with the height of target. We can see that the performance increases with the height of target under the low-grazing scene, where the target height is lower than 600 m [28].

7. CONCLUSIONS

In this paper, we introduce the concept of reflection coefficient considering curved earth effect and the general signal model for MIMO radar in low-grazing angle, and compare the probability of detection of MIMO radar between with multipath and without multipath effects. We further discuss the configuration optimization of phased-array radar and MIMO radar. The simulation results have demonstrated that the performance of detection for MIMO radar is much better than that of phased-radar in low-grazing angle. Based on the analytical results that we derived, we found that for phased-array radar, when the amount of transmitters and receivers are fixed, we should always make the number of transmitters equal to that of receivers; however, the optimal configuration of MIMO radar depends on the signal-to-noise ratio (SNR) heavily.

ACKNOWLEDGMENT

This research is funded in part by the National Natural Science Foundation of China under No. 60872134 and No. 60402032.

REFERENCES

1. Li, J. and P. Stoica, "MIMO radar with colocated antennas: Review of some recent work," *IEEE Signal Process. Mag.*, Vol. 24, No. 5, 106–114, 2007.
2. Haimovich, A. M., R. S. Blum, and L. Cimini, "MIMO radar with widely separated antennas," *IEEE Signal Process. Mag.*, Vol. 21, No. 1, 116–129, 2008.
3. Qu,, Y., G. Liao, S.-Q. Zhu, X.-Y. Liu, and H. Jiang, "Performance analysis of beamforming for MIMO radar," *Progress In Electromagnetics Research*, Vol. 84, 123–134, 2008.
4. Hatam, M., A. Sheikhi, and M. A. Masnadi-Shirazi, "Target detection in pulse-train MIMO radars applying ICA algorithms," *Progress In Electromagnetics Research*, Vol. 122, 413–435, 2012.
5. Chen, J., Z. Li, and C.-S. Li, "A novel strategy for topside ionosphere sounder based on spaceborne MIMO radar with

FDCD," *Progress In Electromagnetics Research*, Vol. 116, 381–393, 2011.

6. Huang, Y., P. V. Brennan, D. Patrick, I. Weller, P. Roberts, and K. Hughes, "FMCW based MIMO imaging radar for maritime navigation," *Progress In Electromagnetics Research*, Vol. 115, 327–342, 2011.
7. Bekkerman, I. and J. Tabrikian, "Target detection and localization using MIMO radars and sonars," *IEEE Trans. on Signal Process.*, Vol. 54, No. 10, 3873–3883, 2006.
8. Forsythe, K., D. Bliss, and G. Fawcett, "Multiple-input multiple-output (MIMO) radar: Performance issues," *38th Asilomar Conf. Signal, Syst., Comput.*, 310–315, Pacific Groove, CA, Nov. 2004.
9. Zhou, W., J. T. Wang, H. W. Chen, and X. Li, "Signal model and moving target detection based on MIMO Synthetic Aperture Radar," *Progress In Electromagnetics Research*, Vol. 31, 311–329, 2012.
10. Stoica, P., J. Li, and Y. Xie, "On probing signal design for MIMO radar," *IEEE Trans. on Signal Process.*, Vol. 55, No. 8, 14151–4161, 2007.
11. Li J. and P. Stoica, Eds., *MIMO Radar Signal Processing*, Wiley, New York, 2008.
12. Lehmann, N., A. Haimovich, R. Blum, and L. Cimini, "Target velocity estimation and antenna placement for MIMO radar with widely separated antennas," *40th Asilomar Conf. Signals, Syst., Comput.*, 25–30, Pacific Groove, CA, 2006.
13. Godrich, H., V. Chiriac, A. Haimovich, and R. Blum, "Target tracking in MIMO radar systems: Techniques and performance analysis," *IEEE Radar Conf.*, 1111–1116, 2010.
14. Fishler, E., A. Haimovich, and R. Blum, "Spatial diversity in radars-models and detection performance," *IEEE Trans. on Signal Process.*, Vol. 54, No. 3, 823–838, 2006.
15. Jin, Y., J. M. F. Moura, and N. O'Donoughue, "Time reversal in multiple-input multiple-output radar," *IEEE Journal of Selected Topics in Signal Processing*, Vol. 4, No. 1, 210–225, 2010.
16. Barton, D. K., "Low angle tracking," *IEEE Proceeding*, Vol. 62, No. 6, 210–225, 1974.
17. Silon, S. L. and B. D. Carlson, "Radar detection in multipath," *IEE Proc. Radar, Sonar and Navigation*, Vol. 146, No. 1, 45–54, 1999.
18. Sen, S. and A. Nehorai, "Adaptive OFDM radar for target detection in multipath scenarios," *IEEE Trans. on Signal Process.*,

Vol. 59, No. 1, 78–90, 2011.

19. White, W., "Low-angle radar tracking in the presence of multipath," *IEEE Trans. on Aerosp. Electron. Syst.*, Vol. 10, No. 6, 835–852, 1974.
20. Mrstik, A. and P. Smith, "Multipath limitations on low-angle radar tracking," *IEEE Trans. on Aerosp. Electron. Syst.*, Vol. 14, No. 1, 85–102, 1978.
21. Bar-Shalom, Y., A. Kumar, W. Blair, and G. Groves, "Tracking low elevation targets in the presence of multipath propagation," *IEEE Trans. on Aerosp. Electron. Syst.*, Vol. 30, No. 3, 973–979, 1994.
22. He, Q., R. Blum, H. Godrich, and A. Haimovich, "Target velocity estimation and antenna placement for MIMO radar with widely separated antennas," *IEEE J. Sel. Topics Signal Process.*, Vol. 4, No. 1, 79–100, 2010.
23. Chen, H. W., X. Li, J. Yang, W. Zhou, and Z. W. Zhuang, "Effects of geometry configurations on ambiguity properties for bistatic MIMO radar," *Progress In Electromagnetics Research B*, Vol. 30, 117–133, 2011.
24. Li, J., L. Xu, P. Stoica, K. W. Forsythe, and D. W. Bliss, "Range compression and waveform optimization for MIMO radar: A Cramer-Rao bound based study," *IEEE Trans. on Signal Process.*, Vol. 56, No. 1, 218–232, 2008.
25. Tang, J., Y. Wu, Y. Peng, and X. Wang, "On detection performance and system configuration of MIMO radar," *Sci. China Ser. F — Inf. Sci.*, Vol. 52, No. 7, 1250–1257, 2009.
26. Lo, T. and J. Litva, "Use of a highly deterministic multipath signal model in low-angle tracking," *IEE Proc. F — Radar and Signal Processing*, Vol. 138, No. 2, 163–171, 1991.
27. Freehafer, J. E., W. T. Fishback, W. H. Furry, and D. E. Kerr, "Theory of propagation in a horizontal stratified atmosphere," *Propagation of Short Radio Waves*, 27–180, McGraw-Hill, 1951.
28. Shirman, Y. D., S. P. Leshchenko, and V. M. Orlenko, "Wideband radar (advantages and problems)," *2004 Second International Workshop*, 71–76, 2004.